Angular distributions of Sc fragments from the interaction of ^{238}U with 0.8–400 GeV protons

D. R. Fortney* and N. T. Porile

Department of Chemistry, Purdue University, West Lafayette, Indiana 47907

(Received 14 January 1980)

Angular distributions of ^{44}Sc^m, ^{46}Sc, ^{47}Sc, and ^{48}Sc emitted in the interaction of ^{238}U with 0.8, 3.0, 11.5, and 400 GeV protons have been measured. The angular distributions peak at forward angles at 0.8 and 3 GeV but are sideward-peaked at 11.5 and 400 GeV. At 400 GeV, fewer fragments are emitted at forward than at backward angles. Isotopic differences were found to be small. The data were fitted with the function $F_L(\theta_L) = 1 + A_1\cos\theta_L + A_2\cos^2\theta_L$ and were also analyzed in terms of the two-step model. The values of A_1 peak at 3 GeV, go through zero at 11.5 GeV, and become negative at 400 GeV. The values of A_2 are zero at 0.8 GeV and become increasingly negative with increasing proton energy. A qualitative explanation in terms of a possible change in the nature of proton-nucleus interactions at high energies is presented.

$$\left[\begin{array}{c} \text{NUCLEAR REACTIONS } {}^{238}\text{U}(p,x) \, {}^{44}\text{Sc}^m, \, {}^{46}\text{Sc}, \, {}^{47}\text{Sc}, \, {}^{48}\text{Sc}. \quad T_p = 0.8, \; 3.0, \; 11.5, \\ 400 \text{ GeV. Measured angular distributions.} \end{array}\right]$$

I. INTRODUCTION

Considerable evidence has accumulated in recent years indicating that a profound change in the mechanism for the formation of light fragments and deep spallation products from the interaction of heavy elements with high-energy protons occurs at energies below 10 GeV. Beg and Porile[1] thus discovered that the ratio of forward-to-backward emission (F/B) of several deep spallation products from the interaction of ^{238}U with protons peaked sharply in the vicinity of 3 GeV while the ranges decreased by about a factor of 2 between 1 and 4 GeV. Similar results were later reported for a broad range of products from the interaction of both uranium and gold with protons.[2–6] These results have been interpreted[5,7] in terms of a change in the initial proton-nucleus interaction from an intranuclear cascade to a coherent interaction with part of the nucleus.[8]

Angular distribution measurements also reveal a striking change in the production of these nuclides at multi-GeV energies. Remsberg and Perry[9] measured the angular distributions of light fragments emitted in the interaction of heavy elements with 28 GeV protons. Sideward peaking was observed for fragments such as sodium in contrast to the forward peaking previously observed at 2.9 GeV.[10] Porile et al.[11] similarly observed that the angular distributions of deep spallation products resulting from the interaction of ^{238}U with 11.5 GeV protons peaked at sideward angles. By contrast, forward peaking had been observed for these products at a bombarding energy of 2.2 GeV.[12,13] In a recent report Porile et al.[14] measured the angular distributions of a number of

products resulting from 400 GeV proton bombardment of uranium. In addition to sideward peaking, these authors also observed several instances of a novel effect, namely, preferential emission at backward angles. This result indicates that measurements at the highest available energies are of special interest.

The present work is one of a series of studies of the variation with proton energy between 0.8 and 400 GeV of the properties of scandium fragments emitted in the breakup of uranium. These products are apparently formed in near-central collisions and a study of their properties may be used to probe nuclear matter under fairly extreme conditions. Previous papers in this series have dealt with the excitation functions and thick-target recoil properties,[3] and with the differential ranges of fragments emitted at 90° to the beam.[15] The excitation functions were found to rise steeply with energy up to ~10 GeV and the recoil properties exhibited the behavior described above. The spectra derived from the differential ranges broadened with increasing proton energy while the peaks shifted to lower values suggesting that extensive mass dissipation occurred prior to breakup for proton energies of 10 GeV and above. We report here the results of angular distribution measurements on ^{44}Sc^m, ^{46}Sc, ^{47}Sc, and ^{48}Sc performed at 0.8, 3.0, 11.5, and 400 GeV. The first three of these energies span the region of the peak in F/B as well as the sharp dropoff in range, while the 400 GeV experiments focus on the unusual enhancement at backward angles.[14] The existence of four measurable isotopes makes it possible to investigate the effect of fragment composition. Preliminary reports of this work have been published.[14,16]

II. EXPERIMENTAL

The experimental procedure has been described in detail in previous reports from our laboratory.[11,15] We emphasize here only those details unique to the present work.

The experiments at 400 GeV were performed in the Neutrino Hall beam line at Fermilab, those at 11.5 and 3.0 GeV in the internal beam of the zero-gradient synchroton (ZGS), and those at 0.8 GeV in line B of LAMPF. The experiments involved the irradiation in vacuum of thin UF_4 targets and the collection of the emitted fragments in aluminum. The targets consisted of 0.1–0.3 mg/cm² UF_4 evaporated onto high-purity aluminum (99.999%) and were inclined at 30° and 150° (ZGS) or 45° and 135° to the beam. The catchers consisted of 50 μm thick 99.999% pure aluminum and were sufficiently thick to stop all the Sc fragments. An additional 25 μm foil backed up the catchers in order to protect them from the possibility of contamination by recoils originating in the catcher holder. The catchers intercepted the angular range of 15°–105° and 75°–165° relative to the beam direction (5°–105° and 75°–175° at Fermilab). In a single ZGS irradiation either the forward or backward half of the angular distribution could be determined. By contrast, at LAMPF and Fermilab measurements over the entire angular range could be performed in a single exposure. This was accomplished by placing two targets back to back with enough aluminum between them to prevent any cross contamination of recoils.

The catcher foils were cut into 15° wide strips (a 10° wide strip was cut at the most forward and backward angles at Fermilab). Because of the low counting rates, the catcher foils subtended a large fraction of the available solid angle. The resulting mismatch between the spherical reaction coordinates and the cylindrical catcher angles dictated that the foils be cut along curves of constant recoil angle for a point source of recoils.[17] The solid angle subtended by each catcher as well as the average recoil angle were evaluated with a code[18] which, in addition to the target-catcher geometry, took into account the beam profile at the target location. This profile was determined from the distribution of the ^{24}Na activity in the target backing. The beam spot varied in full width at half-maximum from ~0.3 cm at Fermilab to 1.0 ×2.2 cm at LAMPF. The solid angles subtended by the catcher segments were approximately 0.3 sr at all energies. This value applies with relatively little variation over most of the angular range excepting the most forward and backward angles, for which much smaller solid angles were available.

The irradiations were performed for periods ranging from ~1 hr (ZGS) to ~1 week (Fermilab). Following bombardment, the Al foils were cut and dissolved and scandium separated by a previously described[3] radiochemical procedure. The samples were assayed with Ge(Li) detectors and results obtained for ^{44}Sc^m, ^{46}Sc, ^{47}Sc, and ^{48}Sc on the basis of the γ rays emitted by these nuclides.[3] The angular distributions were obtained by extrapolation of the counting rates to end of bombardment and correction for chemical yield and solid angle. The forward and backward halves of each angular distribution were combined by normalizing them to each other at their common intervals.

As a check on the forward-backward normalization a number of experiments were performed with the catcher foils in a 2π geometry. The target stack in these experiments consisted of two Al foils in contact, with one foil having ~0.3 mg/cm² UF_4 evaporated onto it. Two such sets of foils, with the target facing forward and backward, respectively, were irradiated in a single experiment. This combination permitted a correction to be made for the small (1–3 %) amount of Sc activity retained in the target.

In order to ensure the validity of the results, two subsidiary types of experiments were performed. The possible contribution to the Sc activities from extraneous sources was investigated in blank experiments performed at each accelerator and upper limits of 1% were placed in all cases. In a different experiment, the effect of target thickness on the angular distribution was investigated at 11.5 GeV. The results obtained for 100 μg/cm² and 300 μg/cm² thick targets yielded essentially identical results indicating that scattering effects could be neglected at these thicknesses.

III. RESULTS

The angular distributions of ^{44}Sc^m, ^{47}Sc, and ^{48}Sc are displayed in Figs. 1–3, respectively. The results for ^{46}Sc are very similar to those obtained for the other isotopes but, due to the long half-life of this nuclide, are subject to greater statistical uncertainty. Either two or three complete angular distributions were measured at each energy and the separate results are displayed. The plotted points are the differential cross sections at the average laboratory angle θ_L normalized to unity at 90°. Typical error bars are shown; these are based on the statistical uncertainties in the counting rates (1–5 %), estimated errors in the determination of solid angles and their dispersion due to finite target size (2–5 %), uncertainty in forward-backward normalization (2%), and error in
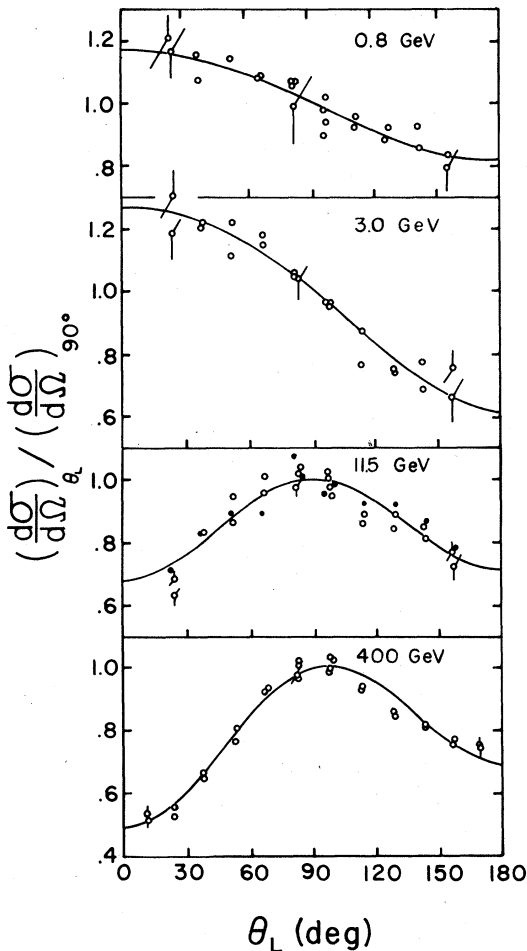
FIG. 1. Angular distributions of $^{44}Sc^m$ from the interaction of ^{238}U with 0.8-400 GeV protons. The various points at each angle represent the results of replicate experiments. The solid points at 11.5 GeV show the results obtained for a "thin" (100 μg/cm^2) target. Typical error bars are shown at each energy. The curves constitute a least-squares fit of Eq. (1). The differential cross sections are normalized to unity at 90°.

chemical yield determination (2%).

In order to systematize the rather large body of data obtained in this study it is useful to fit the laboratory angular distributions with some simple function containing relatively few parameters. It was found that the following two-parameter equation gave a reasonable fit to the data:

$$F_L(\theta_L) = 1 + A_1 \cos\theta_L + A_2 \cos^2\theta_L . \qquad (1)$$

Similar functions, including forms with additional terms in the series, were also tried and found to be less satisfactory. The curves in Figs. 1–3 represent least-squares fits of Eq. (1) to the data points. The resulting values of A_1 and A_2 are summarized in Table I. It is seen that the points
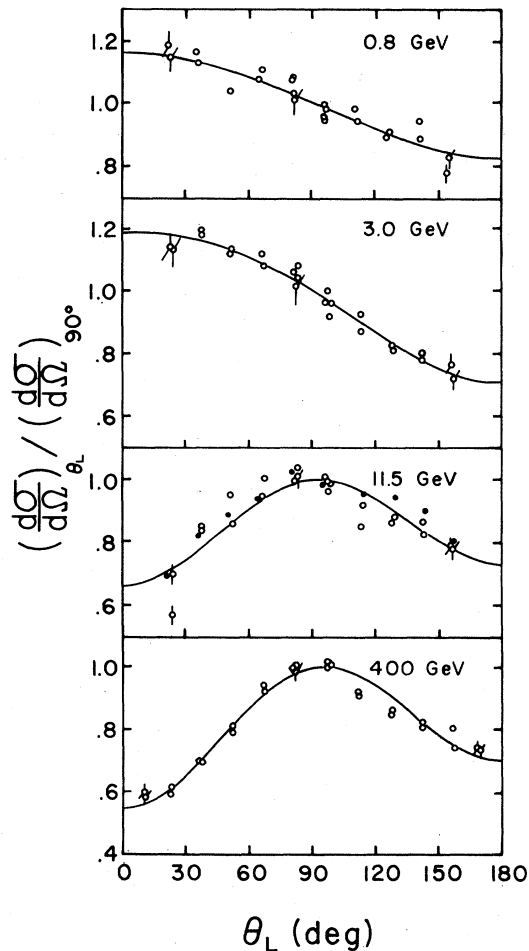

FIG. 2. Angular distributions of ^{47}Sc. See Fig. 1 for details.

generally scatter about the curves in a fairly random way. Note, however, that at 400 GeV, where the greatest precision was obtained, the curves appear to systematically overestimate the values of the differential cross sections in the vicinity of 120° by somewhat more than one standard deviation. The significance, if any, of this discrepancy is unclear at this time.

A useful measure of the asymmetry in the angular distribution is the ratio of forward-to-backward emission, $(F/B)_{\theta_L}$. This quantity may be conveniently obtained by integrating the fitted angular distributions over the forward and backward hemispheres, i.e.,

$$(F/B)_{\theta_L} = \frac{\int_0^{\pi/2} F_L(\theta_L) \sin\theta_L d\theta_L}{\int_{\pi/2}^{\pi} F_L(\theta_L) \sin\theta_L d\theta_L} . \qquad (2)$$

The resulting values are summarized in Table I.

As indicated above, several experiments in which the catchers were in a 2π geometry were
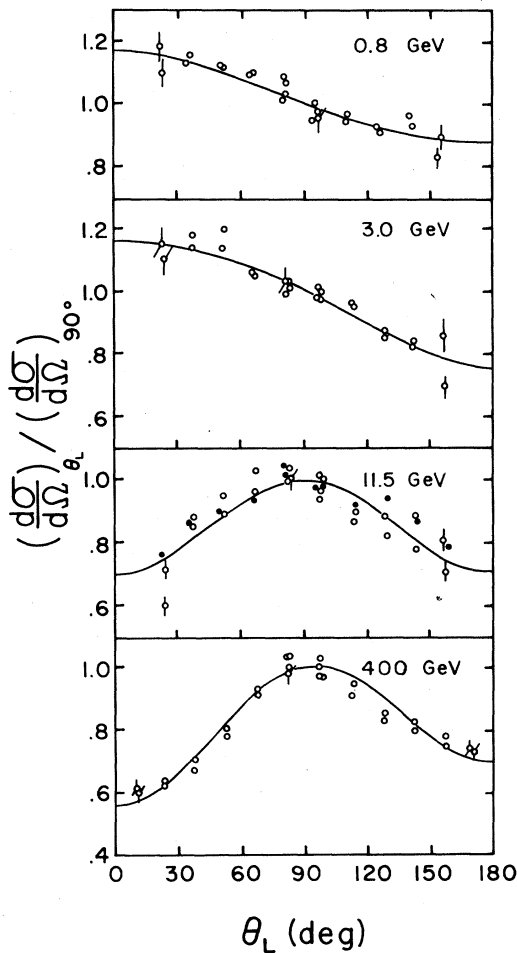
FIG. 3. Angular distributions of ^{48}Sc. See Fig. 1 for details.

performed to check on the forward-backward normalization and recoil retention in the target. These experiments may be used to derive values of the forward-to-backward emission ratio, designated $(F/B)_{2\pi}$, by use of the relation

$$(F/B)_{2\pi} = R_B(R_F + 1)/(R_B + 1) , \qquad (3)$$

where R_B and R_F are the experimental forward-to-backward ratios obtained with the target material evaporated onto the backward and forward catchers, respectively. A single experiment of this type was performed at 3 GeV and replicates were run at 11.5 and 400 GeV. The results are summarized in Table I. It is seen that both types of F/B determinations yield essentially the same values, confirming the validity of the forward-backward normalization. In particular, the values of $(F/B)_{2\pi}$ obtained at 400 GeV are significantly less than unity confirming the rather unusual result derived from the angular distributions at this energy.

IV. DISCUSSION

A. Variation of angular distributions with proton energy and product composition

The results displayed in Figs. 1–3 clearly show that some unusual changes in the nature of highly inelastic interactions occur at multi-GeV energies. The angular distributions thus are forward peaked at 0.8 and 3 GeV, with the asymmetry increasing with proton energy in this regime. This trend is indicative of increasing forward momentum transfer to the struck nucleus, consistent with the high excitation energy transfer implied by the steeply rising excitation functions.[3,19,20] Between 3 and

TABLE I. Parametrization of the angular distribution of Sc fragments from the interaction of ^{238}U with protons.

T_p (GeV)	Nuclide	A_1	A_2	$(F/B)_{\theta_L}$	$(F/B)_{2\pi}$
0.8	^{44}Sc^m	0.178 ± 0.035	-0.010 ± 0.045	1.20 ± 0.04	
	^{46}Sc	0.126 ± 0.044	-0.024 ± 0.064	1.14 ± 0.05	
	^{47}Sc	0.172 ± 0.018	-0.010 ± 0.020	1.19 ± 0.02	
	^{48}Sc	0.152 ± 0.014	0.020 ± 0.017	1.16 ± 0.02	
3.0	^{44}Sc^m	0.324 ± 0.023	-0.062 ± 0.026	1.40 ± 0.03	1.40 ± 0.10
	^{46}Sc	0.220 ± 0.035	-0.152 ± 0.039	1.26 ± 0.04	
	^{47}Sc	0.243 ± 0.015	-0.059 ± 0.018	1.28 ± 0.02	1.46 ± 0.03
	^{48}Sc	0.202 ± 0.018	-0.046 ± 0.020	1.23 ± 0.02	1.16 ± 0.04
11.5	^{44}Sc^m	-0.013 ± 0.019	-0.310 ± 0.026	0.99 ± 0.02	1.00 ± 0.01
	^{46}Sc	-0.041 ± 0.011	-0.239 ± 0.017	0.96 ± 0.01	0.96 ± 0.01
	^{47}Sc	-0.033 ± 0.027	-0.307 ± 0.037	0.96 ± 0.03	1.00 ± 0.01
	^{48}Sc	-0.003 ± 0.029	-0.300 ± 0.039	1.00 ± 0.03	1.01 ± 0.01
400	^{44}Sc^m	-0.100 ± 0.007	-0.411 ± 0.010	0.89 ± 0.01	0.91 ± 0.01
	^{46}Sc	-0.056 ± 0.011	-0.356 ± 0.012	0.94 ± 0.01	0.95 ± 0.02
	^{47}Sc	-0.072 ± 0.008	-0.377 ± 0.011	0.92 ± 0.01	0.95 ± 0.01
	^{48}Sc	-0.064 ± 0.011	-0.374 ± 0.014	0.93 ± 0.01	0.95 ± 0.01

11.5 GeV the angular distributions undergo a major change: Forward peaking gives way to sideward peaking and the angular distributions become symmetric about 90° in the laboratory. This may be indicative of a process in which the energy and momentum of the incident proton are carried off by an ensemble of participant nucleons, with the fragments being formed from the spectator remnant.[5,7] At 400 GeV, the angular distributions retain the prominent peak at 90° but, in addition, show that emission at backward angles is more likely than that at forward angles.[14]

A somewhat different perspective on these trends is provided in Fig. 4, which shows the energy dependence of the parameters A_1 and A_2, as well as that of the forward-to-backward ratio, for each of the Sc fragments. The parameter A_1, which is a measure of the forward-backward asymmetry, initially increases with proton energy, peaks at 3 GeV, and becomes negative at 400 GeV. There is a small but significant difference between the value of A_1 for neutron-deficient $^{44}Sc^m$ and those for the three neutron-excess fragments. The former thus is larger than the latter up to 3 GeV indicating that the angular distribution is more forward peaked. On the other hand, A_1 for $^{44}Sc^m$ is more negative at 400 GeV, reflecting the greater degree of backward enhancement for this frag-

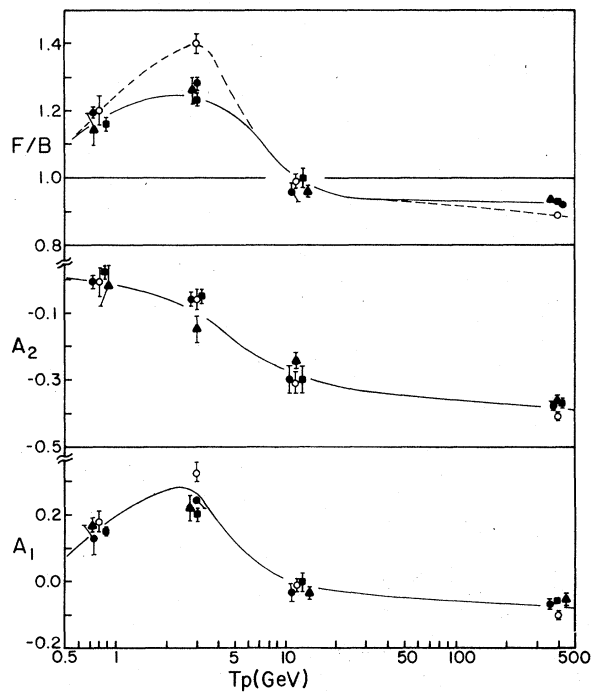ment. The parameter A_2 is a measure of the anisotropy and decreases monotonically with bombarding energy, reflecting the increasing importance of sideward relative to forward-backward emission. Within the limits of error, there is no isotope effect in A_2.

The energy dependence of F/B is similar to that previously obtained in thick-target experiments[3] but the present values are uniformly lower. This difference is a consequence of the fact that the thick-target values are range weighted while the present results are independent of range. As is already apparent in the angular distribution plots, the F/B ratios are less than unity at 400 GeV. The difference in A_1 values between $^{44}Sc^m$ and the other isotopes results in a corresponding difference in F/B, as indicated.

The previously measured excitation functions for the formation of Sc nuclides from ^{238}U (Ref. 3) may be used to convert the angular distributions to differential cross sections (mb/sr). As an example of this procedure we display the values of $d\sigma/d\Omega$ for ^{47}Sc in Fig. 5. It is apparent that the transition from forward to sideward peaking occurs only once the production cross section is close to its maximum value. In order to compare the changes in shape in detail it is more convenient to normalize the differential cross sections to the same value of the integrated cross section at all energies. The results obtained in this fashion for ^{47}Sc are displayed in Fig. 6. It is of interest to note that the angular distributions at backward angles are similar in shape, particularly at the higher energies. The large change in the shapes occurs at forward angles, where the normalized differential cross sections decrease sharply between 3 and 11.5 GeV. The decrease in F/B to
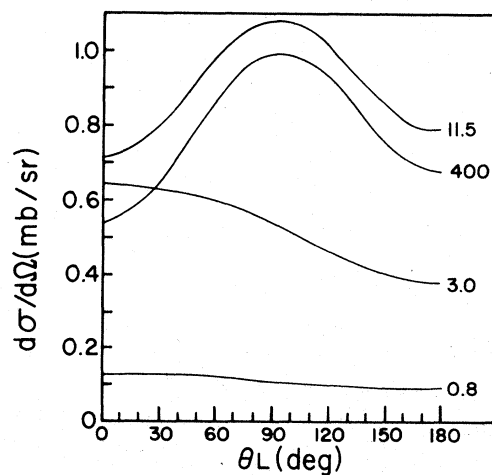

FIG. 4. Energy dependence of angular distribution parameters A_1, A_2, and F/B for $^{44}Sc^m$ (O), ^{46}Sc (▲), ^{47}Sc (●), and ^{48}Sc (■). The curves show the trends in the data.

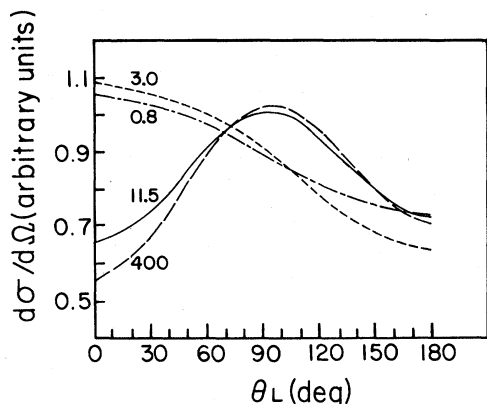FIG. 5. Differential cross sections (mb/sr) of ^{47}Sc at the indicated proton energies.

FIG. 6. Differential cross sections of ^{47}Sc normalized to the same value of the integrated cross section. The numbers near the curves represent the bombarding energies.

below unity at 400 GeV may thus be viewed as a natural continuation of this trend. The differential ranges of Sc fragments[15] indicate that an increasing amount of mass dissipation occurs with increasing proton energy. Recent coincidence experiments performed on fragments emitted in the interaction of ^{238}U with 11.5 GeV protons also show that extensive mass loss occurs prior to fragment emission.[7] An explanation of the backward enhancement may thus be sought in a possible connection between these two trends. If the loss of close to half the mass of the target at 400 GeV (Ref. 15) occurs primarily at forward angles, the nuclear density in the forward cone will be sharply reduced. Furthermore, if fragment emission occurs prior to either equilibration or rotation, the occurrence of such a process at forward angles

must be hindered, thereby leading to the observed relative enhancement at backward angles.

B. Two-step vector model analysis

The angular distributions may be analyzed in terms of the two-step vector model commonly used to interpret high-energy nuclear reactions. Although the general validity of this model above 3 GeV is questionable, it is nonetheless of interest to examine the dependence on energy and isotopic mass of the parameters in the model in view of the large body of data that has been analyzed in this fashion.

Let $\vec{v}$ be the velocity acquired by the struck nucleus as a result of the initial interaction. The components of v along and at right angles to the beam direction are designated $v_{\parallel}$ and $v_{\perp}$, respectively. The effect of $v_{\perp}$ on the angular distributions is small and unduly complicates the analysis.[11,21] We have therefore not incorporated this variable in the present version of the two-step model. The mean velocity acquired by the fragment in the breakup step is denoted as $\vec{V}$ and its angular distribution in the moving frame obeys the relation

$$F(\theta) = \frac{1 + (b/a)\cos^2\theta}{1 + b/3a}, \tag{4}$$

where b/a is the anisotropy parameter. Note that the angular distribution is symmetric about 90° as required by the temporal separation between the two steps. The ratio $\eta_{\parallel} = v_{\parallel}/V$ is a measure of the relative velocity imparted in the two steps and is one of the important parameters derived from the analysis. The laboratory angular distribution may be expressed in terms of $\eta_{\parallel}$ and b/a by the equa-

TABLE II. Two-step model parameters derived from angular distributions of Sc fragments.

T_p (GeV)	Nuclide	$\eta_{\parallel}$	b/a	$1000\beta_{\parallel}$
0.8	^{44}Sc^m	0.089 ± 0.018	−0.023 ± 0.040	5.8 ± 1.2
	^{46}Sc	0.063 ± 0.024	−0.026 ± 0.054	3.9 ± 1.4
	^{47}Sc	0.086 ± 0.008	−0.019 ± 0.022	5.4 ± 0.6
	^{48}Sc	0.076 ± 0.007	0.010 ± 0.017	4.7 ± 0.5
3.0	^{44}Sc^m	0.163 ± 0.010	−0.115 ± 0.028	10.2 ± 0.8
	^{46}Sc	0.111 ± 0.015	−0.214 ± 0.046	6.6 ± 1.0
	^{47}Sc	0.123 ± 0.007	−0.087 ± 0.018	7.4 ± 0.6
	^{48}Sc	0.102 ± 0.008	−0.060 ± 0.021	6.0 ± 0.6
11.5	^{44}Sc^m	−0.003 ± 0.012	−0.311 ± 0.026	−0.2 ± 0.7
	^{46}Sc	−0.021 ± 0.008	−0.240 ± 0.014	−1.1 ± 0.4
	^{47}Sc	−0.013 ± 0.015	−0.308 ± 0.038	−0.7 ± 0.8
	^{48}Sc	0.002 ± 0.014	−0.301 ± 0.036	0.1 ± 0.7
400	^{44}Sc^m	−0.057 ± 0.008	−0.421 ± 0.016	−3.0 ± 0.4
	^{46}Sc	−0.030 ± 0.007	−0.355 ± 0.013	−1.6 ± 0.4
	^{47}Sc	−0.040 ± 0.008	−0.383 ± 0.014	−2.0 ± 0.4
	^{48}Sc	−0.036 ± 0.008	−0.378 ± 0.016	−1.8 ± 0.4

tion[22]

$$F_L(\theta_L) = \frac{1 + (b/a)\cos^2[\theta_L + \sin^{-1}(\eta_{\parallel}\sin\theta_L)]}{1 + b/3a}$$

$$\times \frac{[\eta_{\parallel}\cos\theta_L + (1 - \eta_{\parallel}^2\sin^2\theta_L)^{1/2}]^2}{(1 - \eta_{\parallel}^2\sin^2\theta_L)^{1/2}} \quad . \quad (5)$$

This equation assumes that $\eta_{\parallel} \ll 1$ not only on the average, but for each interaction. The effect of overlapping distributions of $v_{\parallel}$ and V has been discussed elsewhere[23] and does not affect the present analysis.

The parameters obtained from a least-squares fit of Eq. (5) to the data are summarized in Table II. The resulting angular distributions are virtually indistinguishable from the curves in Figs. 1–3 provided that the same normalization is used. This is not surprising since for $\eta_{\parallel} \ll 1$ Eq. (5) reduces to Eq. (1) with $A_1 \simeq 2\eta_{\parallel}$ and $A_2 \simeq b/a$. Table II also lists the mean values of $v_{\parallel}$ (designated $\beta_{\parallel}$ and expressed in units of c) obtained by combining the values of $\eta_{\parallel}$ with the mean velocities derived from the 90° differential range spectra for the same reactions.[15] This procedure assumes that the velocities derived from these spectra can be exclusively associated with the breakup step, an assumption that is approximately valid for small $v_{\perp}$.

The energy dependence of b/a and $\beta_{\parallel}$ is displayed in Fig. 7. The values of b/a show that, within the context of the two-step model, the angular distributions are isotropic in the moving system at 0.8 GeV and become increasingly sideward peaked at higher energies. Within the limits of error, all the Sc fragments display the same values of b/a.
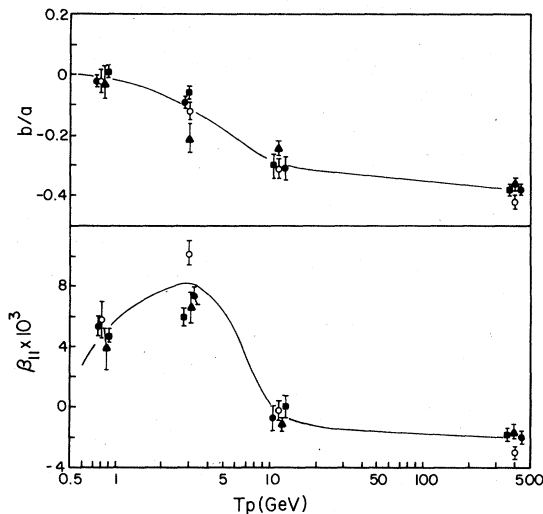

FIG. 7. Energy dependence of two-step model parameters $\beta_{\parallel}$ and b/a for Sc fragments. See Fig. 4 for symbols.

The values of $\beta_{\parallel}$ increase between 0.8 and 3 GeV, drop sharply to zero at 11.5 GeV, and become negative at 400 GeV. According to the two-step model, the residual nucleus resulting from the initial proton-nucleus interaction thus is at rest in the laboratory for a proton energy of 11.5 GeV, and actually recoils backward when the bombarding energy is increased to 400 GeV. These observations are difficult to reconcile with the high excitation energies that appear to be required to form Sc fragments from uranium[3,15] and suggest that the two-step model may not be applicable in these cases. A comparison of the energy spectra of fragments emitted at forward and backward angles would provide a more rigorous test of the consistency of the angular distributions with the two-step model.[10]

V. CONCLUSIONS

The angular distributions of Sc fragments emitted in the interaction of ^{238}U with 0.8–400 GeV protons have been measured. The distributions become increasingly forward peaked between 0.8 and 3 GeV. This trend does not continue at higher energies; instead, the 11.5 GeV curves are sideward peaked and symmetric about 90°. At 400 GeV, the peaking at sideward angles becomes even more pronounced and, in addition, emission at forward angles is less probable than that at backward angles. These features are displayed by both neutron-excess and neutron-deficient fragments.

The results appear to be consistent with a model advanced to explain some related high-energy results.[5,7] In a near-central collision at highly relativistic energies, the Lorentz contraction results in a coherent interaction between the incident proton and the nucleons lying in its path.[8] Owing to relativistic time dilation the resulting multiparticle state is ejected from the nucleus in the forward direction prior to decay. Additional mass loss occurs from the zone adjacent to the ejected tube due to final state interactions, frictional effects, etc. The resulting nucleus is highly unstable and rapidly breaks apart. The fast time scale of the process, which is attested to by the anomalous results obtained from an analysis based on the two-step model, leads to preferential emission at 90° to the beam. Since practically all the momentum of the proton is carried off by the ejected participants, the spectator fragments show little evidence of momentum transfer and so display a forward-to-backward ratio close to unity. A quantitive formulation of this model has been recently published.[24] The backward enhancement observed at 400 GeV can be explained as a conse-

quence of the very extensive mass dissipation observed at this energy.[15] If this process primarily depletes a cone-shaped region of the nucleus opening at forward angles, a rapid breakup will inhibit the emission of fragments at these angles. Since the back side of the nucleus is not depleted, backward emission is not reduced and so is enhanced relative to emission at forward angles. By contrast, the forward peaking seen up to 3 GeV is understandable as the result of the transfer of both momentum and excitation energy to the struck nucleus by the intranuclear cascade.

ACKNOWLEDGMENTS

*Present address: Sandia Corporation, Albuquerque, New Mexico.

[1]K. Beg and N. T. Porile, Phys. Rev. C 3, 1631 (1971).

[2]S. B. Kaufman and M. W. Weisfield, Phys. Rev. C 11, 1258 (1975).

[3]Ø. Scheidemann and N. T. Porile, Phys. Rev. C 14, 1534 (1976).

[4]S. B. Kaufman, E. P. Steinberg, and M. W. Weisfield, Phys. Rev. C 18, 1349 (1978).

[5]S. Biswas and N. T. Porile, Phys. Rev. C 20, 1467 (1979).

[6]D. R. Fortney and N. T. Porile, Phys. Rev. C 14, 1652 (1976).

[7]B. D. Wilkins, S. B. Kaufman, E. P. Steinberg, J. A. Urbon, and D. J. Henderson, Phys. Rev. Lett. 43, 1080 (1979).

[8]G. Berlad, A. Dar, and G. Eilam, Phys. Rev. D 13, 161 (1976); Meng Ta-chung, ibid. 15, 197 (1977); Meng Ta-chung and E. Moeller, Phys. Rev. Lett. 41, 1352 (1978).

[9]L. P. Remsberg and D. G. Perry, Phys. Rev. Lett. 35, 361 (1975).

[10]J. B. Cumming, R. J. Cross, J. Hudis, and A. M. Poskanzer, Phys. Rev. 134, B167 (1964).

[11]N. T. Porile, S. Pandian, H. Klonk, C. R. Rudy, and E. P. Steinberg, Phys. Rev. C 19, 1832 (1979).

[12]V. P. Crespo, J. B. Cumming, and A. M. Poskanzer, Phys. Rev. 174, 1455 (1968).

[13]K. Bächmann and J. B. Cumming, Phys. Rev. C 5, 210 (1972).

[14]N. T. Porile, D. R. Fortney, S. Pandian, R. A. Johns, T. Kaiser, K. Wielgoz, T. S. K. Chang, N. Sugarman, J. A. Urbon, D. J. Henderson, S. B. Kaufman, and E. P. Steinberg, Phys. Rev. Lett. 43, 918 (1979).

[15]D. R. Fortney and N. T. Porile, Phys. Rev. C. 21, 664 (1980).

[16]D. R. Fortney and N. T. Porile, Phys. Lett. 76B, 553 (1978).

[17]C. R. Rudy, N. T. Porile, and S. B. Kaufman, Nucl. Instrum. Methods 138, 19 (1976).

[18]D. R. Fortney, Ph.D. thesis, Purdue University, 1979 (unpublished).

[19]N. T. Porile, Phys. Rev. 120, 572 (1960).

[20]N. T. Porile and N. Sugarman, Phys. Rev. 107, 1422 (1957).

[21]A. M. Poskanzer, J. B. Cumming, and R. Wolfgang, Phys. Rev. 129, 374 (1963).

[22]J. B. Marion, T. I. Arnette, and H. C. Owens, Oak Ridge National Laboratory Report No. ORNL-2574, 1959 (unpublished).

[23]N. T. Porile, Phys. Rev. 185, 1371 (1969); V. P. Crespo, J. B. Cumming, and J. M. Alexander, Phys. Rev. C 2, 1777 (1970); L. Winsberg, Nucl. Instrum. Methods 150, 1465 (1978).

[24]J. B. Cumming, Phys. Rev. Lett. 44, 17 (1980).